Development of a biomimetic liver tumor-on-a-chip model based on decellularized liver matrix for toxicity testing

Siming Lu [1,2,3], Fabio Cuzzucoli [1,2,3,4], Jing Jiang [1,2], Li-guo Liang [1,2,3], Yiming Wang [1,2,3], Mengqi Kong [1,2,3], Xin Zhao [5], Wenguo Cui [6], Jun Li [1,2 #], ShuQi Wang [1, 2, 3 #]

[1] *State Key Laboratory for Diagnosis and Treatment of Infectious Diseases, First Affiliated Hospital, Zhejiang University School of Medicine, Hangzhou, Zhejiang Province, 310003, China*

[2] *Collaborative Innovation Center for Diagnosis and Treatment of Infectious Diseases, Hangzhou, Zhejiang Province, 310003, China*

[3] *Institute for Translational Medicine, Zhejiang University, Hangzhou, Zhejiang Province, 310029, China*

[4] *University of Waterloo, 200 University Avenue West, Waterloo, ON, N2L 3G1, Canada*

[5] *Department of Biomedical Engineering, the Hong Kong Polytechnic University, Hong Kong, China*

[6] *Shanghai Institute of Traumatology and Orthopaedics, Shanghai Key Laboratory for Prevention and Treatment of Bone and Joint Disease, Ruijin Hospital, Shanghai Jiao Tong University School of Medicine, 197 Ruijin 2nd Road, Shanghai 200025, P.R. China*

Corresponding author. E-mail: lijun2009@zju.edu.cn; shuqi@zju.edu.cn

Abstract

Cancer poses a great health threat to both developed and developing countries, and anti-cancer drugs are of important interest for improved clinical outcomes. Although tumor-on-a-chip technologies offer a feasible approach to screening drug toxicity, their capability to mimic the native tumor microenvironment (TME) is still limited. For better mimicry of TME, we developed a biomimetic three-dimensional (3D) liver tumor-on-a-chip with the integration essential components derived from decellularized liver matrix (DLM) with gelatin methacryloyl (GelMA) in a microfluidics-based 3D dynamic cell culture system. The biomimetic liver tumor-on-a-chip based on the integration DLM components with GelMA, as opposed to GelMA only, had an increased capability to maintain cell viability and to enhance hepatocyte functions under flow conditions. The improved performance of the DLM-GelMA-based tumor-on-a-chip may be attributed to the provision of biochemical factors (*e.g.,* growth factors), the preservation of scaffold proteins, and the reestablishment of biophysical cues (*e.g.,* stiffness and shear stress) for better recapitulation of 3D liver TME. Furthermore, this DLM-GelMA-based tumor-on-a-chip exhibited linear dose-dependent drug responses to the toxicity of acetaminophen and sorafenib. Taken together, our study demonstrates that the DLM-GelMA-based biomimetic liver tumor-on-a-chip better mimics *in vivo* TME and holds great promise for a breadth of pathological and pharmacological studies.

Keywords*:* tumor-on-a-chip, decellularization, tumor microenvironment (TME), drug toxicity, 3D culture.

1. Introduction

Globally, liver cancer has become the second leading cause of cancer-related mortality with an incidence rate of nearly 850,000 new cases every year [1]. Despite the clinical severity, few new anti-cancer drugs are readily available, since effective compounds screened by traditional two-dimensional (2D) culture system often fail in animal studies or clinical trials [2, 3]. This is mainly due to the inadequacy of conventional 2D cell culture models, which are unable to mimic complex pathophysiological conditions and predict the toxicity of therapeutic compounds [4, 5]. Although animal models are used as the gold standard for drug testing, these models are expensive and time-consuming, and more importantly they cannot reliably predict the safety and efficacy in clinical studies [2, 6]. As a result, high risks still exist in Stage 1 clinical trials, when drug candidates even pass animal studies, as unknown side effects are often observed [7]. Thus, creating reliable, cost-effective *in vitro* models to facilitate the development of anti-cancer drugs and to compensate for the drawback of conventional models is essential to improve the clinical management of liver cancer.

Recently, organ-on-a-chip models have been used as drug testing platforms due to their close simulation of drug-induced toxicity *in vivo*, a major reason for the withdrawal of drugs [8-11]. Although tumor-on-a-chip technologies offers a feasible approach to drug toxicity testing, their capability to mimic the native extracellular matrix (ECM) is still, to a certain extent, limited [12]. To simulate the mechanical structures of ECM, biomaterials such as hydrogels are used to encapsulate cells for 3D culture [10, 13-15]. For instance, gelatin methacryloyl (GelMA) hydrogels have been commonly used as 3D scaffolds to closely simulate some critical mechanical properties of ECM [16-18]. Although GelMA scaffolds closely resemble the mechanical characteristics of ECM, the *in vitro* 3D culture systems still lack appropriate native growth factors that promote cell growth and sustain cell function [16, 19, 20]. As documented, external growth factors added into GelMA mixtures can effectively facilitate cell growth *in vitro* [13, 18]. Thus, a close simulation of 3D ECM with native

growth factors would be more accurate for assessing drug toxicity.

To establish an ECM with native growth factors, decellularized liver scaffolds have been developed for the preservation of major collagens and growth factors [21]. For example, a decellularized liver scaffold with retained growth factors enhances the culturing of hepatic cells [21-23]. Furthermore, hepatocytes can attach to the ECM components of an acellular scaffold, and they are significantly affected by bioactive molecules (*e.g.*, hepatocyte growth factor (HGF) and basic fibroblast growth factor (bFGF)) preserved in the liver acellular scaffolds [24]. Although a decellularized liver matrix (DLM) allows for a better maintenance of hepatocyte phenotypes such as section of albumin (ALB) and urea *in vitro* [21, 25-27], the incorporation of DLM components into a perfusion-based tumor-on-a-chip platform for better recapitulation of 3D liver tumor microenvironment (TME) has not yet been reported.

In this study, we developed a biomimetic liver tumor-on-a-chip by integrating structural proteins and growth factors derived from DLM with GelMA in a microfluidic 3D dynamic culture system. This biomimetic liver tumor-on-a-chip better recapitulates the 3D liver TME via DLM-GelMA hydrogels with essential scaffold proteins and growth factors, as well as biophysical cues such as stiffness and shear stress. As demonstrated, this DLM-GelMA-based liver tumor-on-a-chip promoted the cell viability and hepatocyte functions (*e.g.,* production of albumin and urea) of HepG2 cells, as opposed to the use of GelMA only, in a pathologically relevant 3D microenvironment. Moreover, this DLM-GelMA-based tumor-on-a-chip demonstrates dose-dependent responses to the toxicity of acetaminophen and sorafenib. Clearly, this biomimetic liver tumor-on-a-chip platform, with the addition of essential collagens and growth factors derived from DLM, can better recapitulate the 3D liver TME, thus offering an important testing platform for assessing drug toxicity.

2. Materials and methods

2.1 Liver preparation

For the preparation of DLM, a total of 60 livers were collected from adult Sprague-Dawley rats weighing 250-300 g, following the animal experimentation protocols described by the Animal Care Ethics Committee of Zhejiang University. The study was approved by the Zhejiang University Experimental Animal Welfare Ethics Committee (ZJU20170787). An intraperitoneal injection of sodium pentobarbital at 50 mg/kg was used to anesthetize the rats, and the abdomens were then cut open. A cannula was subsequently inserted into the portal vein. The portal vein and vena cava were dissected, and the whole liver was removed. Once excised from the rats, the livers were frozen at -80 °C for a minimum of 24 h.

2.2 Decellularization and characterization of DLM

Prior to the decellularization process, the frozen livers were thawed at room temperature, and the cannula in the portal vein was then attached to a peristaltic pump (LongerPump, Baoding, China) to allow for perfusion. The liver was perfused with phosphate buffered saline (PBS) for 1 h at 20 mL/min, and then with 0.1% (w/v) sodium dodecyl sulfate (SDS) for 5 h, , which was followed by 1% (w/v) Triton X-100 for another 30 min. To remove residual nucleic acid, the livers were additionally perfused with 80 U/mL DNase (Sigma-Aldrich, St. Louis, US) and 5 U/mL RNase (Sigma-Aldrich, St. Louis, US) for 30 min at ambient temperature. Finally, the DLM was washed with PBS containing 2% penicillin-streptomycin and 2.5 μg/ mL amphotericin B (Sangon Biotech, Shanghai, China) for 2 h.

The DLM was then characterized using scanning electron microscopy (SEM), residual nucleic acid measurement, and Hematoxylin and eosin (H&E) staining. For SEM imaging, the DLM and native livers were frozen at -20 °C for 24 h and then lyophilized for 48 h. A total of 6 lyophilized samples of DLM and native livers and observed in a Hitachi Model E-1010 scanning electron microscope (Hitachi, Tokyo,

Japan). For residual nucleic acid measurement, the total DNA from using 6 samples of DLM and 6 native liver samples was quantified. First, DNA was extracted from these samples using a TIANamp Genomic DNA Kit (Tiangen Biotech, Beijing, China). Second, the concentrations of DNA were quantified using a NanoDrop spectrophotometer (Thermo Fisher, Waltham, US) and the ratio of DNA to the weight of lyophilized native livers or DLM was calculated.

H&E staining was also utilized to validate the decellularization process. 6 DLM and native liver samples were H&E stained after 4% formalin-fixing, paraffin embedding, and sectioning. For immunofluorescence analysis of the ECM contents within the DLM and native liver tissue, the sectioned samples (n = 6) were stained using rabbit polyclonal anti-collagen type I antibodies (Abcam, Cambridge, UK), rabbit polyclonal anti-collagen type IV antibodies (Abcam, Cambridge, UK), rabbit polyclonal anti-fibronectin antibodies (Abcam, Cambridge, UK), rabbit polyclonal anti-laminin antibodies (Abcam, Cambridge, UK) and then stained with Goat Anti-Rabbit Alexa Fluor®594 antibodies (Abcam, Cambridge, UK). Finally, the nuclear DNA was stained using 40, 6-Diamidino-2-phenylindole dihydrochloride (DAPI) (Sigma-Aldrich, St. Louis, US). Samples were imaged using a fluorescence microscope (Zeiss, Oberkochen, Germany).

2.3 Preparation and characterization of DLM solution

2.3.1 Preparation of DLM solution

The DLM solutions were prepared via enzymatic digestion of DLM. At room temperature, 1 mg of lyophilized DLM powder was digested in 1 mL enzymolysis solution containing 0.5 mg pepsin/0.1 M HCl (Wuhan ColorfulGene Biological Technology Co., Ltd, Wuhan, China) for 72 h with stirring at 250 rpm. After complete digestion, $1/10^{th}$ of the total volume of 1M NaCl/10× PBS was added to stop the reaction, and the pH was then adjusted to 7.0. The DLM solution was sterilized with a sterilizing filter (0.22 μm) and then concentrated approximately 10-fold using Amicon

Ultr-15 3K centrifugal filters (Millipore, Burlington, MA, US).

2.3.2 Characterization of DLM solution

First, the DLM solution was characterized for preserving collagen fibers. To this end, the collagen concentration, before and after being exposed to UV light (365 nm, 30 s), in the DLM (n = 3) and native liver tissue homogenates (n = 3), was measured using a hydroxyproline (HYP) ELISA Kit (Solarbio technology, Beijing, China). Following the manufacturer's instructions, 2 mL of tissue extract (6 mol/L of HCl) was added into each sample and allowed to incubate at 110 ℃ for 6-12 h, and the supernatant was then collected by centrifugation at 16,000 rpm for 20 min at ambient temperature. Then, 60 μL of supernatant or 60 μL of DI water was mixed with chloramine T, followed by incubation at room temperature for 20 min. Lastly, the resulted oxide reacted with p-dimethylaminobenzaldehyde, producing a red compound with a characteristic absorption peak at 560 nm. The ratio of HYP content to dry weight of samples was calculated based on the manufacturer's instructions and then converted to collagen in a ratio of 1:7.2 (HYP: collagen) (Table S1).

Second, the DLM solution was characterized for preserving growth factors. Rat glycosaminoglycan (GAG), HGF, and bFGF ELISA Kits (Wuhan ColorfulGene biological technology Co., Ltd, Wuhan, China) were utilized to quantify the concentration of GAG, HGF and bFGF, before and after being exposed to UV light (365 nm, 30 s), in the DLM (n = 3) and native liver tissue homogenates (n = 3). Following the manufacturer's instructions, a standard curve of GAG, HGF and bFGF was generated. 10 μL of each sample and 40 μL of dilution buffer were mixed with 50 μL of respective HRP-conjugated reagents and then incubated for 30 min at 37 ℃. After rinsing with PBS for 5 times, 50 μL of chromogenic solution A and B were added and incubated for 10 min at 37 ℃. Finally, 50 μL of stop solution was added, and the absorbance was measured using a SpectraMax M5 (Molecular Devices, San Jose, US) at a wavelength of 450 nm. According to their respective standard curve,

the concentrations of GAG, HGF and bFGF were measured, and the ratio of GAG, HGF and bFGF content to dry weight was calculated.

2.3.3 Protein extraction and digestion for MS

Pretreatment of the DLM solution and native liver tissues was performed to allow for the evaluation of the DLM composition using high-performance liquid chromatography coupled to an Orbitrap™ mass spectrometer (HPLC-MS). The samples (n = 3) were reduced with 50mM dithiothreitol (DTT) at 95 °C for 10 min, and then alkylated in darkness with iodoacetamide at ambient temperature for 30 min. Subsequently, the samples were digested with trypsin (Promega, enzyme-to-sample weight ratio of 1:50) at 37 °C for 12h. The digestion was quenched using 10% formic acid (FA). According to the manufacturer's protocol, a ZipTip C18 (P10, Millipore Corporation, Billerica, MA) was used to desalt the digested peptides. The resultant eluent was subsequently dried using a SpeedVac (Thermo Fisher, Waltham, MA, US) and reconstituted in 2% acetonitrile (ACN) containing 0.1% FA.

2.3.4 Proteomic analysis

The desalted samples were injected into a Waters nanoAcquity high performance liquid chromatography (HPLC) in conjunction with an Orbitrap mass spectrometer (HPLC-MS) (Q-Exactive, Thermo Scientific, MA, US). Peptides were loaded into a BEH C18 nanoACQUITY Column (130Å, 1.7 μm, 75 μm × 250 mm) and eluted at 200 nL/min in 0.1% FA over 120 min using an increasing gradient of ACN. A full-mass scan (300-1800 m/z) was carried out at a resolution of 70,000 in an Orbitrap™ mass spectrometer. Subsequent fragmentation at a higher-energy collisional dissociation (HCD) of 27% collision energy was performed on the 20 most intense peaks. The proteomic analysis was performed at a resolution of 35,000 and an isolation width of 2.0 m/z. MaxQuant was used to analyze the acquired raw files against the Rat UniProt protein database (http://www.uniprot.org/).

2.4 Fabrication of 10% (wt) GelMA and DLM-GelMA

To prepare a stock solution of 10% (wt) GelMA, 0.1 g of GelMA with 1 ml ddH_2O was deposited in the ultrasonic cleaner for 10 min to mix thoroughly. Then, the 10% (wt) GelMA stock solution was mixed with different volumes of the DLM solution. The GelMA-DLM solutions were mixed with 1.0% (wt) 2-hydroxy-4'-(2-hydroxyethoxy)-2-methylpropiophenone, a photoinitiator (PI), (Sigma-Aldrich, St. Louis, US). Finally, to crosslink the hydrogel and change the solution state to solid, the DLM-GelMA solutions were exposed to 6.9 mW cm^{-2} UV light (365 nm) for 30 s. For fabrication of 10% (wt) DLM-GelMA with DLM, different volumes of DLM were added. (Detailed information was provided in Table S2). For example, 2:3 DLM-GelMA was composed of 400 μL of DLM solution, 600 μL of 10% (wt) GelMA and 0.01g PI. To encapsulate hepatocytes, HepG2 (1.0×10^7 cells/mL) were encapsulated in the DLM-GelMA solution and then exposed to UV light (wavelength of 365 nm) for 30 s.

2.5 Characterization of GelMA and DLM-GelMA

2.5.1 Pore size

The pore size of GelMA and DLM-GelMA was measured using SEM. 10 % (wt) GelMA and different volume ratios of DLM-GelMA (*i.e.*, 1: 9 DLM-GelMA, 1: 4 DLM-GelMA, 3: 7 DLM-GelMA, 2: 3 DLM-GelMA, 1: 1 DLM-GelMA) were mixed with 1.0% (wt) PI (Sigma-Aldrich, St. Louis, US), and then exposed under 6.9 mW cm^{-2} UV light (365 nm) for 30 s. The GelMA and DLM-GelMA samples were then frozen at -20 °C for 24 h followed by lyophilization for 48 h. The lyophilized samples were observed using a Hitachi Model E-1010 scanning electron microscope (Hitachi, Tokyo, Japan). Finally, the average pore size was analyzed using Image J software.

2.5.2 Young's modulus

Young's modulus, as an indicator of stiffness, was also measured to characterize DLM-GelMA and GelMA only hydrogels. Both hydrogels was prepared into a

cylinder mold with dimensions of of 10 mm in diameter and 9 mm in height. Unconstrained compression and frequency sweep measurements were performed using a mechanical tester (EFL-MT5600, SuZhou Intelligent Manufacturing Research Institute, SuZhou, China), fitted with a custom compression clamp. The hydrogel samples were compressed with a constant strain rate of 1 mm/min. The elastic modulus was calculated based on the slope of the linear portion of the stress-strain curve between 0 and plus 5% of the initial strain. All mechanical characterization was conducted at 37 °C.

2.5.3 Fourier transform infrared (FTIR) spectroscopy

Additionally, FTIR spectra were anlyzed on an FTIR spectrometer (Nicolet 6700, Thermo Scientific, USA). Hydrogel samples were frozen at -20 ℃ for 24 h followed by lyophilization for 48 h. Samples were subsequently grinded into powder. The ground powder and potassium bromide at a ratio of 1:10 were then ground again and pressed into thin slices under an infrared drying lamp. The hydrogel samples were scanned at resolution of 4 mm/s between 400 cm^{-1} and 4000 cm^{-1}.

2.6 Cell viability of HepG2 cells in DLM-GelMA hydrogels

To determine the status of cells in hydrogels, the HepG2 cell viability was measured at different volume ratios of DLM to GelMA (GelMA only, 1: 9 DLM-GelMA, 1: 4 DLM-GelMA, 3: 7 DLM-GelMA, 2: 3 DLM-GelMA, 1: 1 DLM-GelMA) on days 1, 4, and 8. HepG2 cells, at a cell density of 1.0×10^7 cells/mL, were mixed with different ratios of DLM-GelMA (n = 3) and seeded in 96-well plates (50 μL per well). The wells were subjected to UV light (365 nm) for 30 s, and then 100 μL of DMEM medium was added. On days 1, 4, and 8, the cell viability was measured using Cell Counting Kit-8 reagent (MedChem Express, Monmouth Junction, NJ, USA) according to the manufacturer's instructions. Following the incubation with CCK-8 reagent at 37 °C in 5% CO_2 for 5 h, the absorbance was measured at 450 nm.

2.7 Fabrication of poly(dimethylsiloxane) (PDMS) device

First, the device was fabricated using PDMS, a gas permeable hydrophobic elastomer. The PDMS device contained two chambers and a polyethylene terephthalate (PET) membrane for cell culture (Fig. 1B). The master mold of the PDMS device was made by stacking two layers of poly(methyl methacrylate) (PMMA) together via double sided adhesive (DSA). The top PMMA layer, which contains the mold matching the size and shape of the desired microchannel (height = 0.5 mm, area = 90 mm^2, volume = 45 mm^3), and the bottom PMMA layer, which contains the mold matching the size and shape of the desired microchannel (height = 1 mm, area = 60 mm^2, volume = 60 mm^3) (Table S3) were designed using the CorelDraw® system and excised from the PMMA with a laser cutting machine. Once the PMMA master mold was created, it was used to cast these two channels. For device fabrication, the prepolymer PDMS and curing agent was mixed at a 10:1 (weight ratio) and then degassed at ambient temperature for 30 min. The mixture was then cast into the PMMA master mold and cured for 1 h at 80 ºC. The PDMS layer was carefully peeled off from the PMMA master mold after solidification, and then its edges were trimmed for a uniform shape. Four cylindrical holes, each with a diameter of 2 mm, were punched through the top PDMS layer to form two inlets and two outlets. A 10 μm PET membrane (GE Healthcare Life Science, Shanghai, China) was cut to the desired shape and placed onto the top PDMS chamber. After vacuum plasma treatment, the top PDMS layer containing the PET membrane and the bottom PDMS layer were bonded together.

2.8 Seeding and characterization of HepG2 cells in microfluidic devices

Before seeding, the devices were sterilized using 75% ethanol for 24 h and the channels were soaked in 2% penicillin-streptomycin and 2.5 μg/mL amphotericin B (Sangon Biotech, Shanghai, China) for 2 h. The 2:3 DLM-GelMA with 1.0% (wt) 2-hydroxy-4'-(2-hydroxyethoxy)-2-methylpropiophenone (Sigma-Aldrich, St. Louis, USA) was stored at -4 °C until use. HepG2 cells were suspended in DMEM (Gibco, Melbourne, Australia) with 10% fetal bovine serum (FBS) (Gibco, Melbourne,

Australia), at a final concentration of 1.0×10^7 cells/mL. The cell suspension was centrifuged for 2 min at 1,000 rpm and the medium was replaced with 2:3 DLM-GelMA at the same cell density. A 50 µL of HepG2 cells in 2:3 DLM-GelMA was introduced into the bottom chamber of the PDMS device using a pipette and then exposed to UV-light (365 nm) for 30 s. Media was then added into the top chamber and the devices were maintained under a flow rate of 2 µL/h. Silicone tubing (0.5 mm ID × 2.0 mm OD, LongerPump, Baoding, China) was used for all fluidic connections and media perfusion. The microfluidics-based dynamic long-term 3D cell culture, live/dead staining, ALB and urea secretion measurements were conducted for characterization.

The viability of HepG2 cells embedded in the GelMA only and 2:3 DLM-GelMA hydrogels within the microfluidic devices was analyzed using a Live/Dead assay (Dojindo, Kumamoto, Japan) on days 4, 7, 10, 14 and 21, as described by the manufacturer. To prepare a dye solution that would allow for differentiation between live and dead cells, 3 µL of Calcein acetoxymethyl ester (calcein AM) and 3 µL of PI solution were added to 1 mL of PBS. Cells embedded in the hydrogels were subsequently stained by removing the DMEM medium and replacing it with 500 µL of dye solution. The dye-sample mixture was incubated in darkness at 37 °C with 5% CO_2 in an incubator for 1 h. Stained cells were analyzed using a Nikon A1 confocal fluorescence microscope (Nikon, Tokyo, Japan), and the images were then analyzed using ImageJ software to quantify live/dead cells. Finally, the ratio of live cells to the total number of cells was used to determine the cell viability.

To assess hepatocyte function, urea and ALB secretion were quantified. Culture medium samples collected from HepG2-laden GelMA only and HepG2-laden 2:3 DLM-GelMA were harvested on days 7, 14, and 21 with the media refreshed every 7 days. Secreted urea and ALB were quantified using respective ELISA assay kits (BioAssay systems, Hayward, CA, US) according to the manufacturer's instructions.

Measurement was performed in a Multifunctional microplate reader SpectraMax M5 (Molecular Devices, San Jose, US).

2.9 Toxicity testing

For drug-response experiments, HepG2 cells mixed with 2:3 DLM-GelMA or GelMA only were injected into the PDMS device as described above. After incubation at 37 °C with 5% CO_2 for 48 h, the drug toxicity experiments were performed by exposing HepG2 cells continuously to media containing 0.0, 5.0, 10.0 and 20.0 mM of acetaminophen (MedChem Express, Monmouth Junction, NJ, USA) and 0.0, 10.0, 15.0 and 20.0 μM of sorafenib (MedChem Express, Monmouth Junction, NJ, USA) at 2 μL/h for 24 h. Cells were then stained using Live/Dead assay kit as described above and analyzed using a Nikon A1 confocal fluorescence microscope.

2.10 Statistical analysis

This study employed the one-way analysis of variance (ANOVA) to analyze the significance between experimental groups. P value of less than 0.05 was used to determine the significance level.

3. Results

3.1 Characterization of DLM

Liver decellularization was successfully obtained through physical treatment and chemical perfusion based on the optimization of a decellularization protocol as reported before [27]. Following a 9-h decellularization process, rat livers became transparent (Fig. 2A). The immunostaining of the four ECM proteins (*i.e.*, fibronectin, laminin, collagen type I, and collagen type IV) demonstrated that these ECM basement components were preserved after the decellularization process (Fig. 2B). The absence of cells in the DLM was demonstrated by the lack of blue color following the DAPI staining (Fig. 2B). The H&E staining showed a pink eosinophilic staining, indicative of the presence of collagen, whereas there was no basophilic

staining within the DLM, indicative of the absence of nucleus or cells (Fig. 2C). SEM imaging revealed a mesh-like structure of the DLM (Fig. 2D). DNA quantification results showed the total of DNA after decellularization was 21.99 ± 1.34 ng/mL, suggesting that DNA from the native liver were removed by decellularization and DNase treatment (Fig. 2E). These results demonstrated that the removal of the liver cells was successfully achieved through an optimized decellularization protocol, resulting in DLM within 9 h.

3.2 Characterization of DLM solution

As shown in Fig. 3A, the DLM was freeze-dried into a milky white scaffold, cut into cubes, homogenized with pepsin enzymolysis, and then concentrated using ultrafiltration. The concentration of collagen, GAG, HGF, and bFGF within the DLM solution was measured, and the effect of UV exposure on the degradation of these components was investigated (Fig. 3B-D). Compared to the collagen concentration in native liver tissue, the dry concentration of collagen in the DLM was increased by approximately 18-fold (Fig. 3B and Table S4). The concentration of collagen from the DLM solution before and after UV irradiation was 144.33 ± 50.74 ng/mg, and 147.84 ± 23.71 ng/mg, respectively, indicating that the collagen was not affected by UV exposure ($p > 0.05$). The concentration of GAG from the DLM solution was also increased by 2.5-fold (Fig. 3C and Table S4), compared to its counterpart in native liver tissues. Similarly, the UV exposure did not seem to affect the concentration of GAG within the DLM solution.

The concentration of HGF and bFGF was also measured in the DLM solution, and compared between before and after UV exposure (Fig. 3D and Table S4). The concentration of HGF in the native liver was 6.70 ± 0.08 pg/mg, whereas it decreased to 4.27 ± 0.05 pg/mg (before UV exposure) and 4.37 ± 0.04 pg/mg dry weight (after UV exposure). These data indicate that the decellularization and enzymolysis process reduced the HGF content, and the UV exposure did not seem to affect the

concentration of HGF. The concentration of bFGF the native liver was 5.29 ± 0.09 pg/mg, whereas it was 4.58 ± 0.11 pg/mg in the DLM solution, suggesting a significant loss of bFGF during the decellularization and enzymolysis processes. Furthermore, the concentration of bFGF within the DLM solution reduced to 4.07 ± 0.02 pg/mg, as opposed to 4.58 ± 0.11 pg/mg, after UV exposure, suggesting that UV exposure might damage bFGF. Nevertheless, the majority of HGF and bFGF were preserved within the DLM solution, and the majority of them sustained after UV exposure.

Furthermore, proteomic analysis by MS was sought to investigate the protein components preserved in the DLM solution. The protein profile of the DLM solution was generated by cross-referencing the MS results with the proteome database of *Rattus norvegicus*. The results showed that a large proportion of cellular proteins and debris were removed from the native liver, as shown in the heatmap (Fig. 3E), during the decellularization and enzymolysis processes. In addition, the protein abundance in the DLM solution did not differ substantially before and after UV exposure. As revealed in the pie chart (Fig. 3F), the proportion of protein components in the DLM solution was determined to be 43% ECM-affiliated proteins, 29% glycoproteins, 14% collagens, 7% ECM regulators, and 7% secreted factors. The proteomic analysis revealed that bioactive substances such as collagens, ECM-associated proteins and glycoproteins, as well as growth factors were successfully preserved in the DLM solution.

3.3 Characterization of DLM-GelMA hydrogels

DLM-GelMA, which was fabricated by mixing the DLM solution with 10% GelMA as briefly indicated in Table S2, was characterized with respect to the morphology, mechanical property and infrared fingerprint (Fig. 4A-D). Following UV exposure, the mixture of DLM with GelMA solution became gellified, and the obtained DLM-GelMA biomaterial exhibited porous microstructures under SEM (Fig. 4A).

Notably, the largest pore sizes were observed in DLM-GelMA with a mixing ratio of 2:3 and 1:1, ranging from 100.34 ± 8.56 to 101.54 ± 5.97 μm (Fig. 4B and Table S5). It is also notable that the addition of DLM in GelMA increased the smoothness of DLM-GelMA hydrogels (Fig. 4A), which might be caused by the retention of ECM proteins and growth factors on the surface of GelMA polymers.

The mechanical property of DLM-GelMA hydrogels was characterized by measuring Young's modulus. The results showed that the Young's modulus of the 2:3 DLM-GelMA hydrogels was 16.91 ± 0.54 kPa, which showed no significant difference among the hybrid hydrogels with different mixing ratios and GelMA only (Fig. 4C and Table S5), indicating that the integration of DLM does not significantly alter the Young's modulus of GelMA. In addition, FTIR spectroscopy was used to elucidate the infrared fingerprints of DLM-GelMA in comparison to GelMA and gelatin (Fig. 4D). The results showed that the bands exhibited at ~1650cm^{-1} for gelatin, GelMA, and DLM-GelMA, corresponding to C=O carbonyl stretching from carboxamide linkages. The broad band at 3000-3500cm^{-1} corresponded to OH groups on all three substrates. The new bands at ~1550cm^{-1} for DLM-GelMA and GelMA hydrogels were formed by the symmetric and asymmetric stretching of the carboxylate anion products from the polymerization of GelMA. Clearly, the integration of DLM into GelMA changed the infrared spectrum of GelMA.

3.4 Biocompatibility of DLM-GelMA hydrogels

The biocompatibility of DLM-GelMA was evaluated for culturing HepG2 cells in 3D culture in a 96-well plate. HepG2 cells (1.0×10^7 cells/mL) were seeded into DLM-GelMA hydrogels with different volume ratios to obtain the highest cell viability. As shown in Fig. 4E, the cell viability of HepG2, as indicated by the absorbance of CCK-8 reagent at 450 nm, was the highest on day 1, 4 and 8 , for the DLM-GelMA hydrogels at a volume ratio of 2:3. This volume ratio showed superior cell viability of HepG2 to the second best ratio of 1:1 during the period of 8 days of

cell culture. Evidently, the cell viability of HepG2 cells in the group of DLM-GelMA, regardless of the volume ratio, showed significantly elevated cell viability than the group with GelMA only. Taken together, DLM-GelMA hydrogels showed great biocompatibility with 3D culture of HepG2 cells, and the 2:3 DLM-GelMA hydrogels showed the superior performance. Thus, the 2:3 DLM-GelMA was subsequently chosen for assembling the liver tumor-on-a-chip for further analysis.

3.5 Liver tumor-on-a-chip for long-term 3D cell culture

The effects of DLM on encapsulated HepG2 cells within the 2:3 DLM-GelMA hydrogel was evaluated on a liver tumor-on-a-chip platform. Since the cells were grown in 3D hydrogels with continuously flow of media, HepG2 cells were able to be cultured over a period of 21 days without reducing cell viability, which was measured via live/dead staining with the aid of confocal imaging (Fig. 5A). More importantly, HepG2 viability was significantly elevated due to the addition of DLM components in the hybrid DLM-GelMA hydrogels for up to 7 days (Fig. 5B). There was no significant difference in cell viability during the 3D dynamic culture till Day 21. In addition, the secretion of urea from HepG2 cells encapsulated in the 2:3 DLM-GelMA hydrogels was consistently higher than that in the control group with GelMA only over the entire 21 days of 3D dynamic cell culture on-chip (Fig. 5C). In contrast, the secretion of albumin from HepG2 cells encapsulated in the 2 : 3 DLM-GelMA hydrogels showed significantly higher performance till Day 14 (Fig. 5D). Taken together, these results clearly indicated the superiority of the 2:3 DLM-GelMA hydrogels, compared to the control group with GelMA only, in supporting cell growth and hepatocyte function of HepG2 cells on the liver tumor-on-a-chip platform.

3.6 Toxicity testing based on the liver tumor-on-a-chip

The biomimetic liver tumor-on-a-chip was utilized to assess its capability of toxicity testing. Cell viability and hepatocyte function such as secretion of urea and albumin were measured over increasing concentrations of two model drugs (*i.e.,*

acetaminophen and sorafenib) in the liver tumor-on-a-chip (Fig. 6). The overlaid confocal images of live/dead staining showed that the acetaminophen treatment at 5.0, 10.0 and 20.0 mM resulted in significant cell death after 24 h, compared to the untreated group (Fig. 6A). The respective live/dead images are shown in (Fig. S1-2). A more evident toxic effect was observed for 10.0, 15.0, 20.0 μM of sorafenib treated HepG2 cells in the liver tumor-on-a-chip (Fig. 6A). A similar trend of toxicity arising from acetaminophen and sorafenib was also observed in the liver tumor-on-a-chip with GelMA only (Fig. S3). Furthermore, linear dose-dependent drug responses were observed for both model drugs in terms of cell viability, and urea and albumin secretion (Fig. 6B-G). The linearity of R^2 showing the positive correlation between drug concentration and HepG2 cells is shown in Fig. 6B-G. Compared to GelMA only in the liver tumor-on-a-chip, the performance of 2:3 DLM-GelMA consistently had higher performance regarding cell viability and hepatocyte function (Fig. 6B-G). These results demonstrated the capability of this biomimetic liver tumor-on-a-chip for toxicity testing. More importantly, this biomimetic liver tumor-on-a-chip with integrated structural proteins and growth factors derived from DLM, which is more similar to *in vivo* situations, might have more accurate assessment of drug toxicity.

4. Discussion and conclusion

Although tumor-on-a-chip technologies offer a feasible approach to screening drug toxicity, their capability to highly mimic the native TME is still limited. In this study, we developed a biomimetic liver tumor-on-a-chip platform by incorporating essential bioactive components and growth factors derived from DLM with GelMA in a perfusion-based 3D microfluidic culture system to better recapitulate the liver 3D TME (Fig. 1). Through a decellularization process, liver cells were removed, and DLM with essential collagens (*e.g.*, collagen I, collagen IV, fibronectin, and laminin) and growth factors (HGF and bFGF) was preserved (Fig. 2-3). The incorporation of bioactive extracellular components derived from DLM and growth factors with GelMA not only provided a similar biomechanical ECM (*e.g.*, Young's modulus)

with native liver tissues (Fig. 4), but also increased the viability and function of HepG2 cells *(e.g*., secretion of albumin and urea) in the liver tumor-on-a-chip (Fig. 5). In addition, this biomimetic tumor-on-a-chip with integration of DLM-GelMA, as opposed to GelMA only, maintained a relatively higher level of cell viability and hepatocyte function in the presence of increasing concentrations of acetaminophen and sorafenib (Fig. 6). Therefore, the novel DLM-GelMA-based liver tumor-on-a-chip further improves the recapitulation of the liver 3D TME with essential components derived from DLM and the mimicry of biophysical cues, which holds great potential for more accurate toxicity testing.

In this study, we improved the mimicry of the liver 3D TME in a perfusion-based microfluidic system in three aspects, *i.e.,* scaffolds, biochemical factors and biophysical cues, which have been emphasized for reconstructing liver ECM *in vitro* [13]. To obtain the native liver scaffolds *in vivo*, we first removed cells within a rat liver through sequential perfusion of detergents such as SDS and Triton X-100, to preserve the scaffolds that native liver cells reside. As demonstrated, the major collagen components of liver scaffolds (*e.g.,* collagen I, collagen IV, fibronectin, and laminin) were preserved after decellularization (Fig. 2), which plays an essential role in tumor growth and metastasis [28, 29]. Although the collagen dry weight of the DLM solution is 18-fold that of the native liver (Fig. 3B), the collagen concentration in the device (0.0591 μg/μL) closely resembles the collagen content in the native liver (0.06275 μg/μL) (Detailed calculation can be found in Supporting Information in Table S1). In addition to the scaffold collagens, the decellularization preserved growth factors (HGF and bFGF) as revealed by ELISA (Fig. 3B-D), which have been reported to enhance cell viability and growth *in vitro* [22, 30]. Furthermore, multiple ECM-associated proteins and collagens are preserved, as revealed by mass spectrometry analysis (Fig. 3F). Therefore, we simulated the scaffolds and biochemical factors of the 3D liver TME by providing physiologically relevant concentrations of scaffold proteins and growth factors in the biomimetic liver tumor-on-a-chip platform.

We also simulated the 3D liver TME by reestablishing similar biophysical cues such as stiffness and shear stress as *in vivo* with the aid of 3D DLM-GelMA cell culture in a microfluidic system. With respect to stiffness, we integrated scaffold proteins and growth factors into GelMA, a widely used biomaterial in tissue engineering with a tunable stiffness. The Young's modulus of 2:3 DLM-GelMA was determined to be 16.91± 0.54 kPa (Table S5), which better resembles the Young's modulus of a fibrotic liver (> 12kPa) [31], a pre-condition for liver cancer, and which falls in the range of liver stiffness (ranging approximately from 5 to 60kPa) [15, 32]. Additionally, the 2:3 DLM-GelMA hydrogels had an average pore size 100.34 ± 8.56 μm, which could promote cellular spreading and cell-to-cell interaction, and thus facilitate the formation of extensive 3-D cellular network. Furthermore, we simulated the shear stress that liver cells experience by providing fluidic flow. A flow rate of 2 μL/h in this microfluidic device not only creates a fluid-flow environment for cells, but also constantly facilitates mass exchange (*e.g.,* delivery of oxygen and nutrients and removal of metabolic wastes). The fluid flow is of particularly importance for the DLM-GelMA hydrogel, which has a thickness of 1 mm, since 200 micrometers is reported to be the maximal diffusion distance of oxygen [33]. Hence, the reconstructed 3D liver TME by supplementing GelMA with scaffold proteins and growth factors derived from DLM in a perfusion-based microfluidic chip better recapitulate the 3D liver TME with respect to scaffolds, biochemical factors and biophysical cues.

In addition to liver 3D TME modeling *in vitro*, we optimized the protocol for removing cells from an intact organ to preserve structured proteins and growth factors, a key advance in achieving decellularization for liver regenerative medicine. Via sequential perfusion of SDS and Triton X-100, translucent acellular liver matrices were obtained in 9 h, offering a more efficient way than the method outlined by Uygun *et al.*, which takes almost 72 h to obtain a decellularized liver [27]. Immunofluorescence (Fig. 2B) and H&E staining results (Fig. 2C) confirmed that all

the cells were completely removed from the liver tissues. Moreover, the amount of double stranded DNA (dsDNA) found on the decellularized liver was less than 50 ng/mg of the ECM dry weight (Fig. 2E), which is low enough to meet decellularization requirements [34]. More importantly, acellular scaffolds preserved the four major structural proteins (*i.e.*, collagen I, collagen IV, fibronectin and laminin) of ECM and growth factors (Fig. 3). In our hands, this decellularization protocol has been successfully used to remove cells from heart and kidney (not published). Thus, this optimized decellularization protocol is efficient and versatile in achieving decellularized matrix while maintaining ECM proteins and growth factors for regenerative medicine.

Via the technical advances mentioned above, a major biological finding from this study is that the integration of DLM-based liver-specific growth factors and collagens in a microfluidic system significantly enhanced the viability and function of HepG2 cells. As clearly identified in Fig. 2 and Fig. 3 scaffold proteins such as collagen I, collagen IV, fibronectin, and laminin, and HGF/bFGF are preserved. In addition, other ECM-affiliated proteins, ECM glycoproteins, and ECM regulators are preserved along with some secreted factors after decellularization and enzymolysis (Fig. 3E). The protein components derived from DLM are believed to play an important role in supporting cell growth and sustain hepatocyte function (Fig. 4E and Fig. 5), since addition of growth factors can boost cell growth and functions [22, 30]. However, it should be noted that the difference in supporting cell growth tapers off during long-term culture from Day 10 to Day 21. The major reason is most likely due to the consumption or removal of growth factors from the microfluidics system, since the media was changed at an interval of 7 days. Additionally, it is possible that the perfusion might slowly remove the growth factors from the 3D construct, which can also mitigate the cell viability and hepatocyte function over time. These data suggest that addition of grow factors may be needed to maintain high viability and hepatocyte function in the 2:3 DLM-GelMA hydrogels over a long period of time. Nevertheless,

the secretion of urea and albumin from the DLM-GelMA chip is significantly higher than GelMA only for up to 21 and 14 days, respectively. These data altogether demonstrate that essential ECM components and liver-specific factors derived from DLM contribute to the proliferation and functionality of HepG2 cells in the biomimetic liver tumor-on-a-chip with better recapitulation of the 3D liver TME.

The capability of this biomimetic liver tumor-on-a-chip to screening drug toxicity is also explored using model drugs such acetaminophen and sorafenib. Although hepatotoxicity testing in general can be performed in 3D Transwell or 2D petri dish models, the evident technological advances of this biomimetic liver tumor-on-a-chip would be able better recapitulate liver 3D TME for more accurate toxicity assessment. Indeed, the cell viability decreased in the presence of incresing cencentrations of both model drugs as indicated in confocoal images of live/dead staining (Fig. 6A and Fig. S3), which is also supported by a previous study [35]. Furthermore, linear dose-dependent drug responses were observed in cell viability and hepatocyte function such as secretion of urea and albumin for both acetaminophen and sorafenib (Fig. 6B-G). More importantly, the level of cell viability and hepatocyte functions in the 2:3 DLM-GelMA hydrogels were elevated, compared to GelMA only, in the biomimetic tumor-on-a-chip, suggesting that this DLM-GelMA based biomimetic liver tumor-on-a-chip better recapitulate the *in vivo* liver 3D TME for more accurate toxicity assessment. However, it should be noted that the consumption or depletion of growth factors over long-term culture would not affect the toxicity testing, which was completed in 3 days.

In conclusion, we have developed a novel biomimetic liver tumor-on-a-chip with integration of DLM-based structural proteins and growth factors with GelMA for better recapitulation of the 3D liver TME. The preservation of DLM-associated structural proteins and live-specific growth factors enhanced cell viability and elevated hepatocyte function. In addition, the biomimicry of 3D liver TME with

aspect to structural scaffolds and biophysical cues in a microfluidics-based dynamic 3D cell culture system would contribute to better reestablishment of 3D liver TME *in vitro* to a higher degree. Thus, this biomimetic liver tumor-on-a-chip offers a better *in vitro* disease model or testing platform for a breadth of pathological and pharmacological studies.

Competing Interests

The authors have declared that no competing interests.

Acknowledgments

Dr. Wang would like to acknowledge the supports from the National Key Research and Development Program (2016YFC1101302) and the National Science and Technology Major Project (2018ZX10732401-003-007) from Ministry of Science and Technology of the People's Republic of China.

We obtained HepG2 cells from Chinese Academy of Sciences, Shanghai, China.

References:

1. J. M. Llovet, J. Zucman-Rossi, E. Pikarsky, B. Sangro, M. Schwartz, M. Sherman and G. Gores, *Nature Reviews Disease Primers*, 2016, **2**, **DOI:** 10.1038/nrdp.2016.18.
2. G. Caponigro and W. R. Sellers, *Nature Reviews Drug Discovery*, 2011, **10**, 179-187.
3. H. Qi, G. Huang, Y. L. Han, W. Lin, X. Li, S. Wang, T. J. Lu and F. Xu, *Critical Reviews In Biotechnology*, 2016, **36**, 20-31.
4. A. M. Ghaemmaghami, M. J. Hancock, H. Harrington, H. Kaji and A. Khademhosseini, *Drug discovery today*, 2012, **17**, 173-181.
5. M. H. Wu, S. B. Huang and G. B. Lee, *Lab Chip*, 2010, **10**, 939-956.
6. J. W. Scannell, A. Blanckley, H. Boldon and B. Warrington, *Nature Reviews Drug Discovery*, 2012, **11**, 191-200.
7. H. P. Shih, X. Zhang and A. M. Aronov, *Nature reviews. Drug discovery*, 2018, **17**, 78.
8. S. H. Au, M. D. Chamberlain, S. Mahesh, M. V. Sefton and A. R. Wheeler, *Lab Chip*, 2014, **14**, 3290-3299.
9. S. N. Bhatia and D. E. Ingber, *Nature Biotechnology*, 2014, **32**, 760-772.
10. N. S. Bhise, V. Manoharan, S. Massa, A. Tamayol, M. Ghaderi, M. Miscuglio, Q. Lang, Y. Shrike Zhang, S. R. Shin, G. Calzone, N. Annabi, T. D. Shupe, C. E. Bishop, A. Atala, M. R. Dokmeci and A. Khademhosseini, *Biofabrication*, 2016, **8**, 014101.
11. W. Asghar, R. El Assal, H. Shafiee, S. Pitteri, R. Paulmurugan and U. Demirci, *Materials today*, 2015, **18**, 539-553.
12. H. F. Tsai, A. Trubelja, A. Q. Shen and G. Bao, *Journal of the Royal Society, Interface*, 2017, **14**.
13. J. Zhang, X. Zhao, L. Liang, J. Li, U. Demirci and S. Wang, *Biomaterials*, 2018, **157**, 161-176.
14. J. Wang, F. Chen, L. Liu, C. Qi, B. Wang, X. Yan, C. Huang, W. Hou, M. Q. Zhang, Y. Chen and Y. Du, *Biomaterials*, 2016, **91**, 11-22.
15. D. Dong, T. Hao, C. Wang, Y. Zhang, Z. Qin, B. Yang, W. Fang, L. Ye, F. Yao and J. Li, *Biomaterials*, 2018, **157**, 149-160.
16. D. Loessner, C. Meinert, E. Kaemmerer, L. C. Martine, K. Yue, P. A. Levett, T. J. Klein, F. P. Melchels, A. Khademhosseini and D. W. Hutmacher, *Nature protocols*, 2016, **11**, 727-746.
17. B. H. Lee, H. Shirahama, M. H. Kim, J. H. Lee, N. J. Cho and L. P. Tan, *NPG Asia Mater.*, 2017, **9**, 11.
18. X. Zhao, S. Liu, L. Yildirimer, H. Zhao, R. Ding, H. Wang, W. Cui and D. Weitz, *Advanced functional materials*, 2016, **26**, 2809-2819.
19. F. F. Fu, L. R. Shang, F. Y. Zheng, Z. Y. Chen, H. Wang, J. Wang, Z. Z. Gu and Y. J. Zhao, *ACS Appl. Mater. Interfaces*, 2016, **8**, 13840-13848.
20. Y. Liu and M. B. Chan-Park, *Biomaterials*, 2010, **31**, 1158-1170.
21. S. F. Badylak, D. Taylor and K. Uygun, *Annual Review Of Biomedical Engineering,* 2011, **13**, 27-53..

22. K. M. Park, K. H. Hussein, S. H. Hong, C. Ahn, S. R. Yang, S. M. Park, O. K. Kweon, B. M. Kim and H. M. Woo, *Tissue engineering. Part A*, 2016, **22**, 449-460.
23. X. Liu, L. Zhou, X. Chen, T. Liu, G. Pan, W. Cui, M. Li, Z. P. Luo, M. Pei, H. Yang, Y. Gong and F. He, *Materials science & engineering. C, Materials for biological applications*, 2016, **61**, 437-448.
24. J. E. Arenas-Herrera, I. K. Ko, A. Atala and J. J. Yoo, *Biomedical materials*, 2013, **8**, 014106.
25. O. Barakat, S. Abbasi, G. Rodriguez, J. Rios, R. P. Wood, C. Ozaki, L. S. Holley and P. K. Gauthier, *Journal Of Surgical Research*, 2012, **173**, E11-E25.
26. S. Sabetkish, A.-M. Kajbafzadeh, N. Sabetkish, R. Khorramirouz, A. Akbarzadeh, S. L. Seyedian, P. Pasalar, S. Orangian, R. S. H. Beigi, Z. Aryan, H. Akbari and S. M. Tavangar, *Journal Of Biomedical Materials Research Part A*, 2015, **103**, 1498-1508.
27. B. E. Uygun, A. Soto-Gutierrez, H. Yagi, M.-L. Izamis, M. A. Guzzardi, C. Shulman, J. Milwid, N. Kobayashi, A. Tilles, F. Berthiaume, M. Hertl, Y. Nahmias, M. L. Yarmush and K. Uygun, *Nature Medicine*, 2010, **16**, 814-U120.
28. K. R. Levental, H. M. Yu, L. Kass, J. N. Lakins, M. Egeblad, J. T. Erler, S. F. T. Fong, K. Csiszar, A. Giaccia, W. Weninger, M. Yamauchi, D. L. Gasser and V. M. Weaver, *Cell*, 2009, **139**, 891-906.
29. T. R. Cox, D. Bird, A. M. Baker, H. E. Barker, M. W. Y. Ho, G. Lang and J. T. Erler, *Cancer Res.*, 2013, **73**, 1721-1732.
30. W. Yang, Q. Y. Chen, R. P. Xia, Y. J. Zhang, L. Shuai, J. J. Lai, X. L. You, Y. Jiang, P. Bie, L. D. Zhang, H. Y. Zhang and L. H. Bai, *Biomaterials*, 2018, **177**, 52-66.
31. R. G. Wells, *Biochimica Et Biophysica Acta-Molecular Basis Of Disease*, 2013, **1832**, 884-890.
32. E. C. Beck, M. Barragan, M. H. Tadros, S. H. Gehrke and M. S. Detamore, *Acta biomaterialia*, 2016, **38**, 94-105.
33. L. Corstorphine and M. V. Sefton, *Journal Of Tissue Engineering And Regenerative Medicine*, 2011, **5**, 119-129.
34. P. M. Crapo, T. W. Gilbert and S. F. Badylak, *Biomaterials*, 2011, **32**, 3233-3243.
35. C. Ma, L. Zhao, E. M. Zhou, J. Xu, S. Shen and J. Wang, *Analytical chemistry*, 2016, **88**, 1719-1727.

Legends:

Fig. 1 Schematic of DLM-based liver tumor-on-a-chip and its application for drug toxicity testing. (A) Depiction of the steps used for the fabrication of DLM solution from a native liver. (B) 3D schematic of the device's components (top and bottom layer, top and bottom microchannel, PET membrane, inlets and outlets) and their respective dimensions. (C) Schematic of HepG2-laden DLM-GelMA in a microfluidics device. The hydrogel precursors are injected into a microfluidic device using a pipette and photopolymerized upon UV exposure to form HepG2-laden DLM-GelMA for subsequent drug screening.

Fig. 2 Characterization of the whole liver matrix before, during, and after decellularization. (A) Images of rat livers during perfusion with decellularization reagents at the 0, 1, 6, 6.5 and 9 h of decellularization. (B) Immunofluorescence staining collagen I (red), collagen IV (red), fibronectin (red) and laminin (red) in native liver and DLM. Sections were counterstained with DAPI (blue). (C-D) Comparison of rat livers before and after decellularization. (C) H&E staining of DLM, and (D) SEM images of DLM. (E) DNA quantification of rat livers throughout the decellularization process at 0, 1, 6, 6.5 and 9 h (n = 6). Scale bar: 100 μm (B-C) and 50 μm (D). (Avg ± SE, * stands for $p < 0.05$, NS indicates $p > 0.05$).

Fig. 3 Characterization and biocompatibility of DLM solution before and after UV as opposed to native liver. (A) Timeline and process for fabrication of DLM solution. Content of (B) Collagen, (C) GAG, (D) HGF and bFGF in the native liver, DLM solution and DLM after UV light irradiation using ELISA kits (n = 3). (E) Heatmap of native liver (n = 2), DLM solution (n = 3) and DLM-UV light (n = 3) showing changes in protein abundances under these three conditions. Numbers in the color code are log-transformed-corrected Label-free Quantification (LFQ) intensity. (F) Relative proportion of protein components within the DLM solution as analyzed by mass spectrometry (MS) and proteomics analysis (n = 3). (Avg ± SE, * stands for $p < 0.05$, NS indicates $p > 0.05$).

Fig. 4 Characterization of DLM-GelMA hydrogels. (A) Pore size and structure within tissue microarchitecture in (a) GelMA only, (b) 1:9 DLM-GelMA, (c) 1:4 DLM-GelMA, (d) 3:7 DLM-GelMA, (e) 2:3 DLM-GelMA, (f) 1:1 DLM-GelMA. (I) Scale bar: 50μm and (II) scale bar: 20μm. (B) Average pore size at different ratios of DLM-GelMA analyzed with ImageJ (n = 100). (C) Young's modulus at different ratios of DLM-GelMA (n = 3). (D) FTIR spectra of gelatin, GelMA, and 2:3 DLM-GelMA (n = 3). (E) Cell viability in different ratios of DLM-GelMA hydrogels using CCK-8 kit (n = 3). (Avg ± SE, * stands for $p < 0.05$, NS indicates $p > 0.05$).

Fig. 5 Functional characterization of HepG2-laden DLM-GelMA hydrogels in the tumor-on-a-chip. (A) Live/dead staining showing HepG2 cells embedded in the 10% GelMA/ 2:3 DLM-GelMA hydrogels at day 7, 14 and 21 of cell culture. Due to the uniform distribution within the device, the images were taken from a local region in the DLM-GelMA hydrogel (width: 1,272.79 μm, height: 1,272.79 μm, and depth: 200 μm). Scale bar: 100 μm. (B) Quantification of HepG2 cell viability at day 4, 7, 10, 14, and 21 (n = 3). (C, D) Analysis of (C) urea and (D) ALB concentrations in the 2:3 DLM hydrogels compared to GelMA only (n = 3). (Avg ± SE, * stands for $p < 0.05$, NS indicates $p > 0.05$).

Fig. 6 Evaluation of acetaminophen/sorafenib-induced hepatotoxicity using the tumor-on-a-chip platform with embedded 3D HepG2-laden 2:3 DLM-GelMA hydrogels. (A) Live/dead staining showing acetaminophen (0.0, 5.0, 10.0, and 20.0 mM) and sorafenib (0.0, 10.0, 15.0 and 20.0 μM) treatment of HepG2 embedded in 2:3 DLM-GelMA hydrogels for 24 h. Due to the uniform distribution within the device, the images were taken from a local region in the hybrid DLM-GelMA hydrogel (width: 1,272.79 μm, height: 1,272.79 μm, and depth: 200 μm). Scale bar: 100 μm. (B-G) Does-dependent drug responses between cell viability/hepatocyte function (secretion of urea and albumin) and acetaminophen (B-D) or sorafenib (E-G). Data are presented as Avg ± SE.

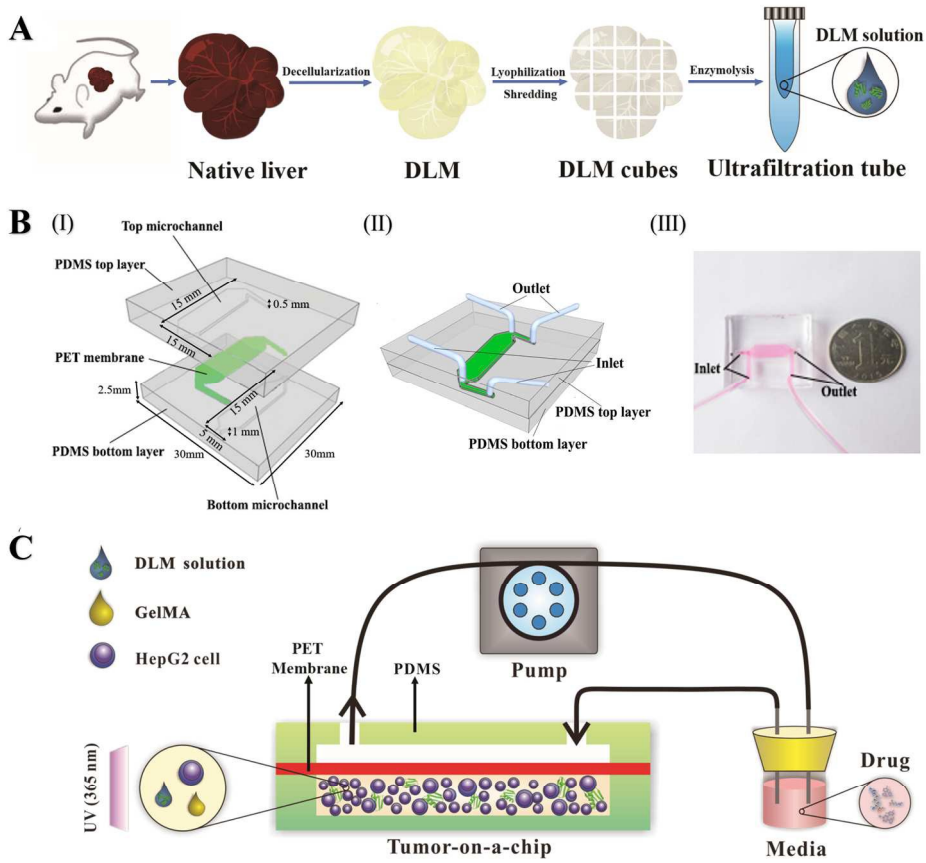

Fig. 1

209x190mm (300 x 300 DPI)

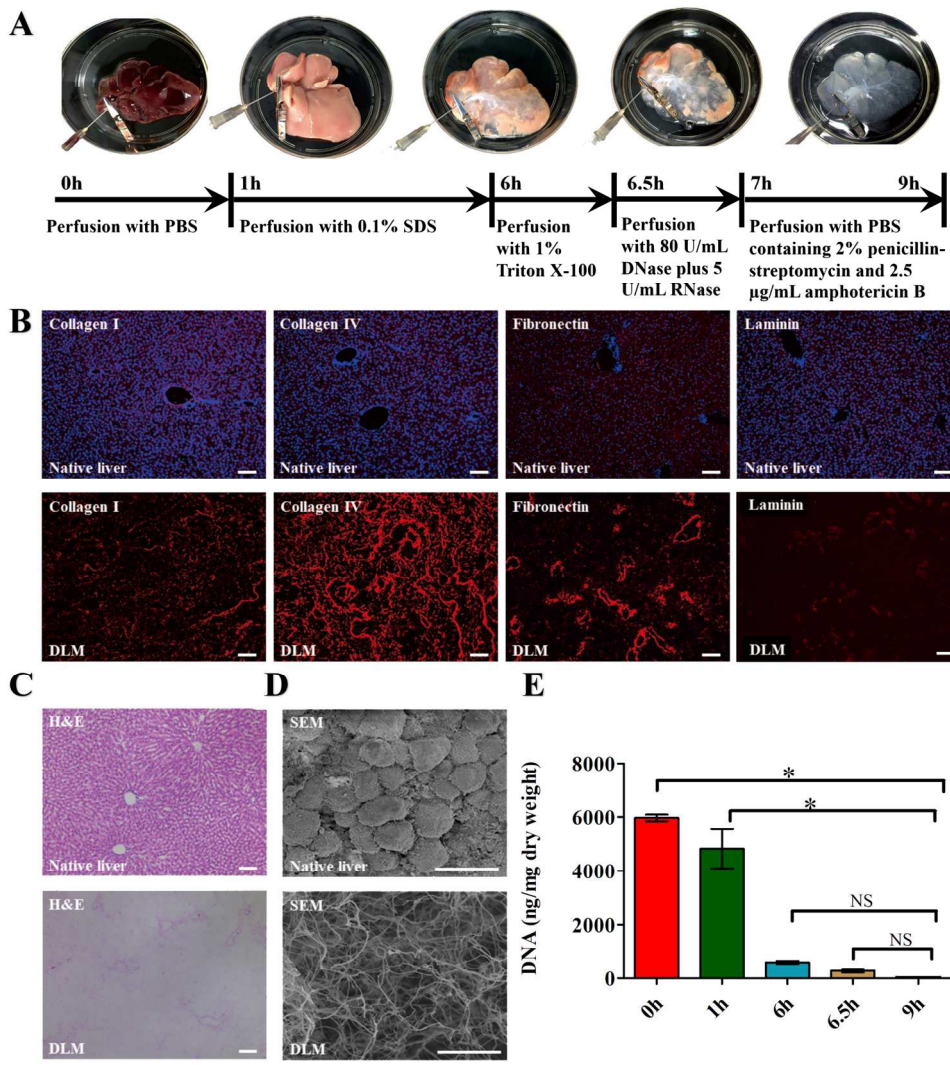

Fig. 2

209x226mm (300 x 300 DPI)

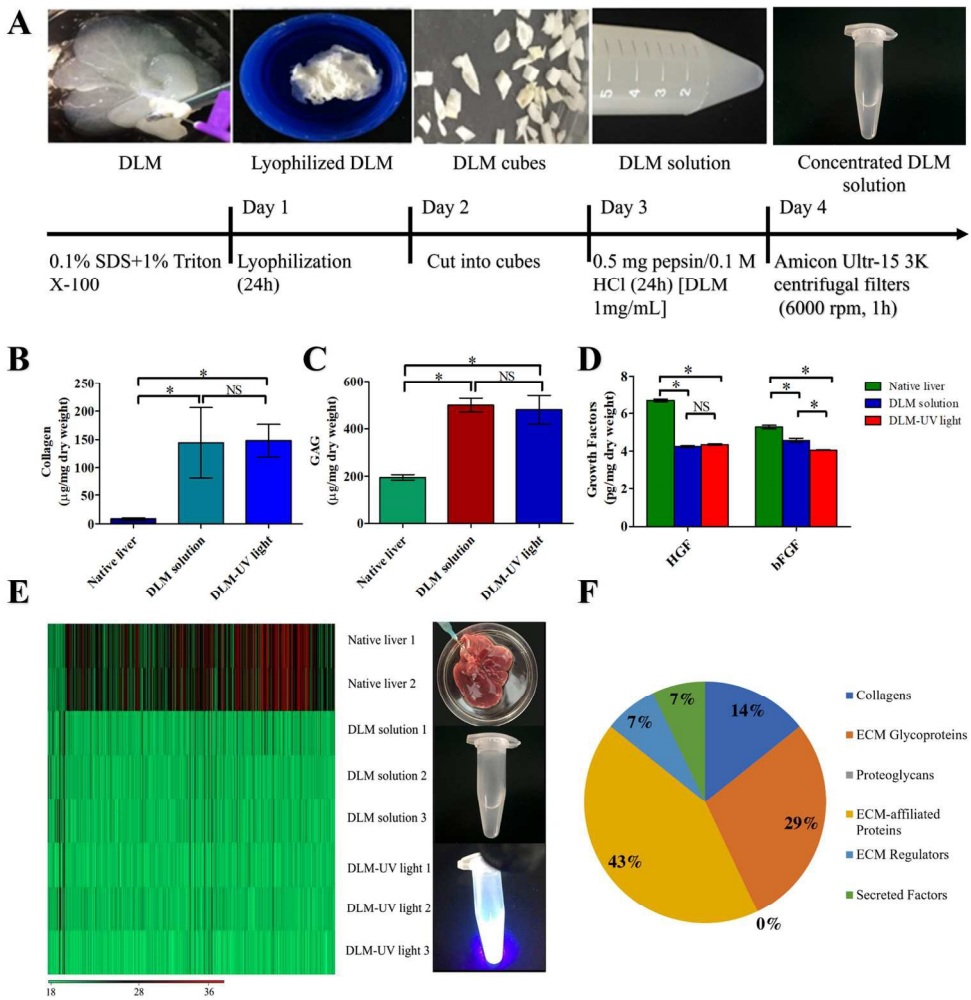

Fig. 3

209x218mm (300 x 300 DPI)

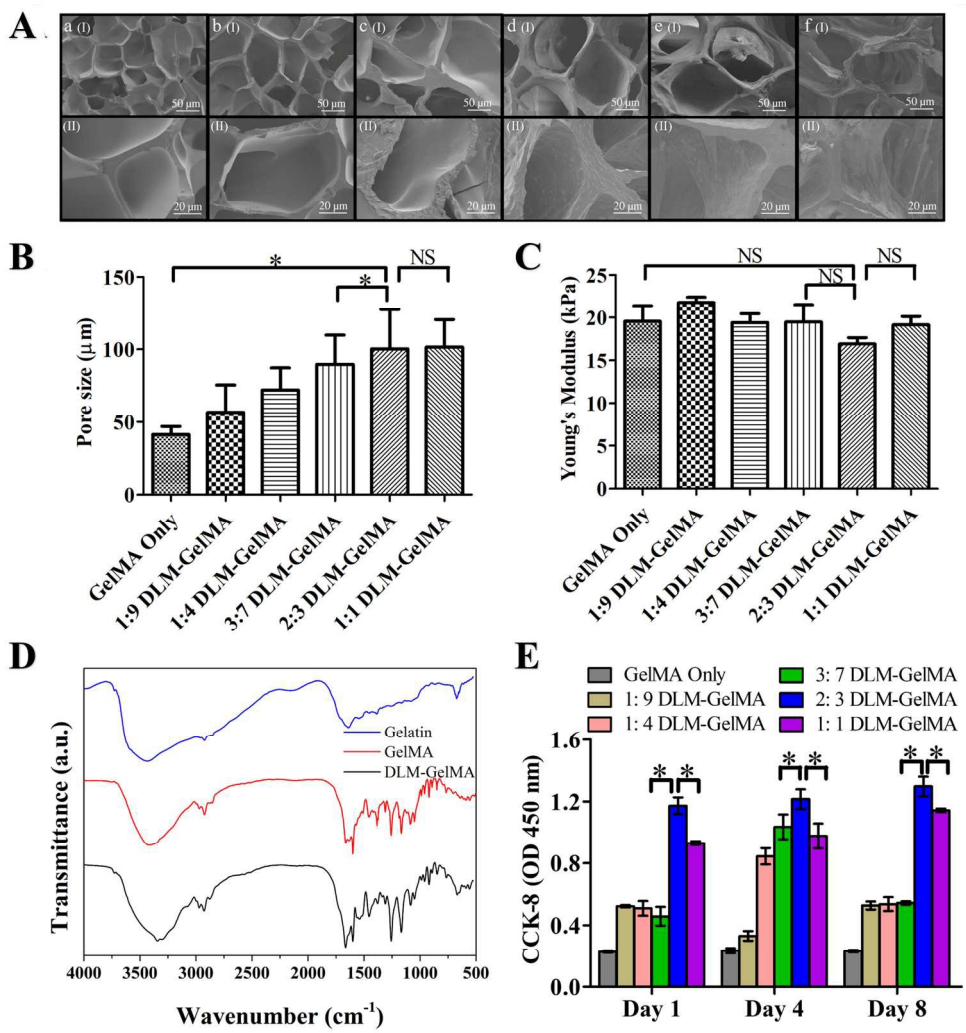

Fig. 4

209x224mm (300 x 300 DPI)

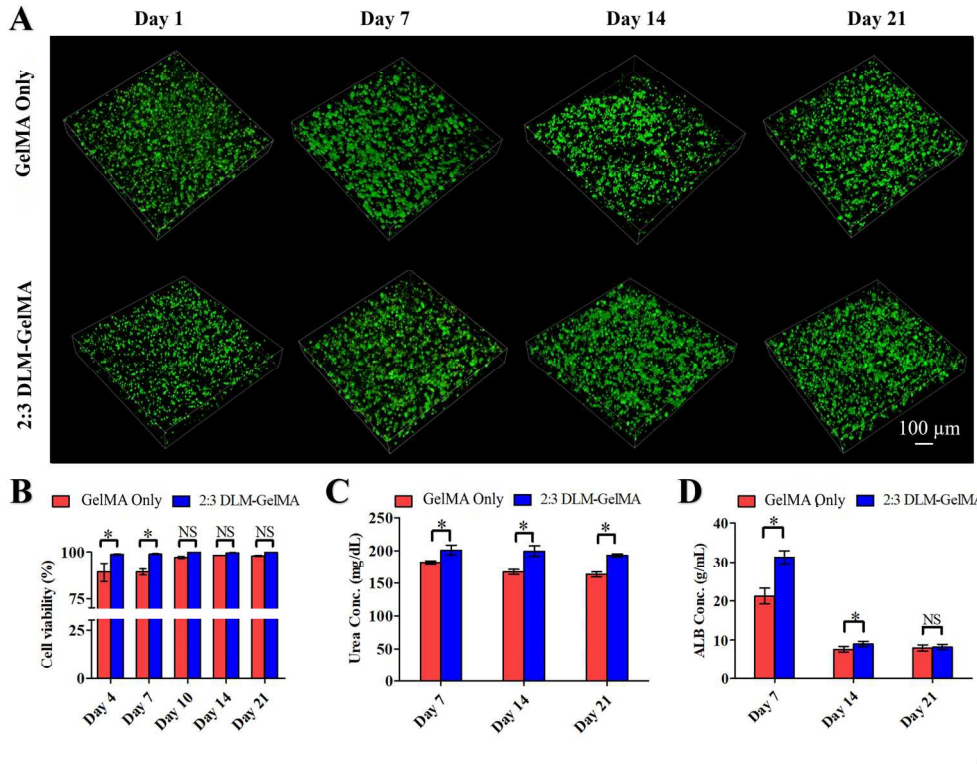

Fig. 5

209x166mm (300 x 300 DPI)

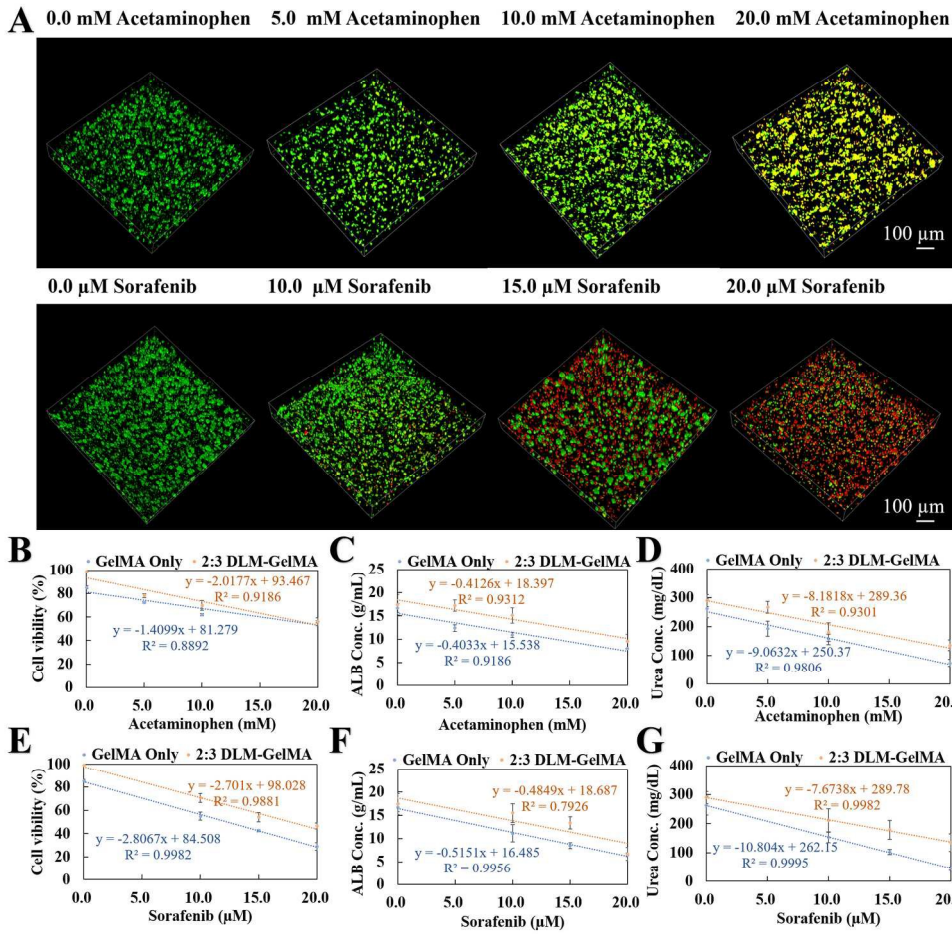

Fig. 6

209x206mm (300 x 300 DPI)